Performance of an *ab initio* equation of state for magnesium oxide

2004 J. Phys.: Condens. Matter 16 5435

(http://iopscience.iop.org/0953-8984/16/30/006)

INSTITUTE OF PHYSICS PUBLISHING JOURNAL OF PHYSICS: CONDENSED MATTER

J. Phys.: Condens. Matter **16** (2004) 5435–5442 PII: S0953-8984(04)79019-0

Performance of an *ab initio* equation of state for magnesium oxide

Sheng-Nian Luo[1,4], Damian C Swift[1], Roberta N Mulford[2], Neil D Drummond[3,5] and Graeme J Ackland[3]

[1] P-24 Plasma Physics, Los Alamos National Laboratory, Los Alamos, New Mexico 87544, USA
[2] NMT-15, Los Alamos National Laboratory, Los Alamos, New Mexico 87544, USA
[3] Department of Physics and Astronomy, University of Edinburgh, Edinburgh EH9 3JZ, UK

E-mail: sluo@lanl.gov

Received 5 April 2004
Published 16 July 2004
Online at stacks.iop.org/JPhysCM/16/5435
doi:10.1088/0953-8984/16/30/006

Abstract

A thermodynamically complete *ab initio* equation of state (EOS) for MgO was obtained using electron density functional theory and the quasiharmonic phonon approximation, and adjusted to match the ambient density. This EOS was demonstrated to be consistent with isotherm, thermal expansivity, heat capacity and melting curve measured in static experiments, and reproduced density and temperature measurements under shock wave loading of bulk and porous periclase. The Grüneisen parameter of periclase at a given density was shown to be weakly dependent on temperature. The B1–B2 phase change was calculated to occur near 320 GPa on the principal Hugoniot. The melting locus of periclase, relevant to the Earth's lower mantle pressures, was predicted to be accessible by shock wave loading of porous periclase, which could also put pressure and temperature bounds on B1–B2 transitions.

1. Introduction

Understanding the structure, composition and evolution of the Earth depends strongly on our knowledge of phase equilibria and equations of state (EOS) of candidate minerals (e.g. silica, MgO periclase and $MgSiO_3$ perovskite) at the pressure (P) and temperature (T) conditions appropriate to the Earth's deep interior. While room temperature high pressure experiments in diamond-anvil cells (DAC) routinely reach megabar pressures, high-temperature DAC experiments with laser or resistance heating remain challenging. Shock wave techniques serve as an essential complement to static techniques by achieving high

[4] Author to whom any correspondence should be addressed.
[5] Present address: Cavendish Laboratory, University of Cambridge, Cambridge, CB3 OHE, UK.

pressure and temperatures simultaneously; they also avoid difficulties with non-hydrostatic stresses in DACs. Theoretically, quantum-mechanics-based calculations yield EOS with improving accuracies. These three techniques are complementary, with their own advantages and disadvantages, and integrated investigations of EOS are necessary.

MgO plays potentially important roles in the physics and chemistry of the lower mantle of the Earth, and in related seismology and geodynamics. MgO has a simple B1 (NaCl-type) structure at low pressures, and its polymorphic change to B2 (CsCl-type) was predicted at pressures above 300 GPa or more at temperatures below 5500 K [1–4]. As existing experiments were probably restricted to the single-phase (B1) regime, it is desirable to compare them with theoretical predictions. In particular, shock wave experiments (including shock temperature measurements) on bulk and porous periclase [5–8] have probed a wide P–V–T space of states (V being specific volume) complementary to static experiments [9–11]. In this work, we compare our thermodynamically complete *ab initio* EOS against static and dynamic experiments, and against another EOS constructed using different techniques and assumptions [12] when applicable. We also investigated the temperature dependence of the Grüneisen parameter because of its convenience for reducing and interpreting data from high-pressure experiments (in particular shock wave experiments). The melting curve of MgO has been measured in DAC up to only about 35 GPa, and remains controversial in comparison with predictions from molecular dynamics simulations [2, 13]. We discuss a realistic experimental approach to resolving the solid–liquid transition at pressures up to about one megabar, in which it is also possible to resolve the B1–B2 boundary.

2. Equation of state

For a crystalline solid at finite temperatures, the Helmholtz free energy and pressure can be regarded as being composed of a contribution from the electron ground states for a perfect lattice at $T = 0$, and thermal contributions from electrons and phonons.

We have predicted single-phase EOS, and thus phase diagrams, by calculating quantum mechanical electron ground states for different lattice parameters with the density functional method in the generalized gradient approximation, using pseudopotentials to represent ions, and a plane-wave basis set [14]. For MgO, calculations were performed using the CASTEP program [15]. The ionic cores were accounted for using ultrasoft Vanderbilt pseudopotentials [16] in Kleinman–Bylander form [15]. The wavefunctions of the valence electrons were expanded in a plane-wave basis set up to an energy cutoff of 540 eV. A single unit cell and a single cubic primitive cell were used in simulations of B1 and B2 phases, respectively. The Brillouin zone was sampled at 20 special points from an $8 \times 8 \times 8$ mesh for a B1 phase using the Monkhorst–Pack scheme [17], while 35 special points from a $9 \times 9 \times 9$ mesh were adopted for a B2 phase.

At finite temperatures, the normal modes of lattice vibrations were calculated using the quasiharmonic approximation, and the lattice-thermal energy was obtained by populating the normal modes according to Bose–Einstein statistics. With pressure and internal energy (E) calculated at various volumes and temperatures, a thermodynamically complete EOS was determined as a pair of tables $P(V, T)$ and $E(V, T)$. The details of the procedure have been presented previously [14]. This procedure was applied to MgO, and the B1–B2 phase boundary constructed from the EOS of the individual phases by equating the Gibbs free energy; further details have been reported elsewhere [4].

The ambient density predicted from the purely *ab initio* EOS for MgO was 3.41 g cm^{-3}, about 5% lower than the experimental value of 3.58 g cm^{-3} for single crystals [7]. A discrepancy of this order is not uncommon for such predictions, but this is a large discrepancy

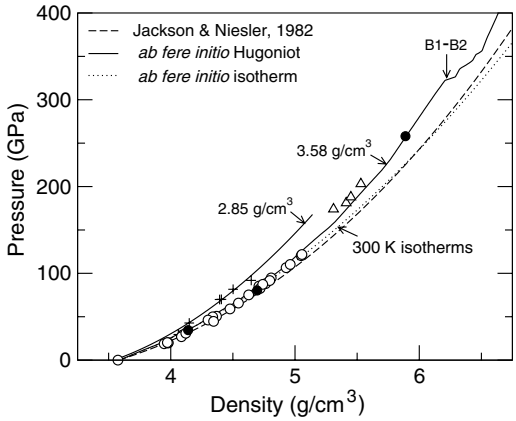

Figure 1. Comparison of the *ab fere initio* EOS with static [9] and shock wave experiments [5–8] in P–ρ space. The experimental 300 K isotherm is the third order Birch–Murnaghan EOS [19] with ambient density of 3.58 g cm^{-3}, bulk modulus of 160.3 GPa and its pressure derivative of 4.13 [9].

compared with the accuracy of experimental data, so correction is desirable. Following the procedure developed previously [14, 18], a pressure offset (tilt in the energy–volume relation) was applied so as to reproduce the ambient density; this was termed *ab fere initio*. For MgO, the pressure shift necessary was 8.1 GPa.

The 300 K isotherm predicted from this *ab fere initio* EOS was in good agreement with the third-order Birch–Murnaghan formulation [19] of quasistatic compression measurements [9, 10], differing by about 1% at the same pressure (figure 1). These results agree with other *ab initio* calculations [12] using the all-electron technique and different pseudopotential schemes. Complementing static data at room temperature, shock wave experiments on bulk and porous periclase [5–8] can better check the validity of the thermal EOS by exploring states in which both pressure and temperature were elevated.

The principal Hugoniot can be constructed from Rankine–Hugoniot (RH) conditions [20] for conservation of mass, momentum and energy across a steady shock. These equations can be closed given an EOS of the form $P(V, E)$; this can be obtained from our thermodynamically complete EOS by eliminating T. At a given shock V, we search for E until the RH conditions are satisfied, and thus obtain the Hugoniot state (V, E, P, T), and the corresponding shock wave velocity U_s and particle velocity u_p. As seen from figures 1–3, the predicted principal Hugoniot was in good accord with experimental results in P–ρ ($\rho \equiv 1/V$), U_s–u_p and P–T spaces [5–8]: the densities at a given pressure differed by about 1% and temperatures within 3%. The differences between prediction of our EOS and experiment in ρ at a given P, when mapped to U_s at a given u_p, became more pronounced at low pressures than high pressures. (This can be explained by error propagations according to RH relations.) As an example, we constructed a U_s–u_p curve (dashed curve in figure 1) from a fictitious P–ρ Hugoniot 1% denser than the principal Hugoniot from *ab fere initio* calculations, and it reproduces the experimental data at low and high pressures (figure 1). The comparison in P–T space (figure 3) is extremely encouraging. This is the first time that an EOS generated by this method has been compared against shock temperature measurements. Temperatures obtained for shocks in transparent (or translucent) materials [8, 21] such as periclase are generally much easier to obtain and more accurate than for opaque materials, thus lending experimental support to the *ab fere initio* EOS.

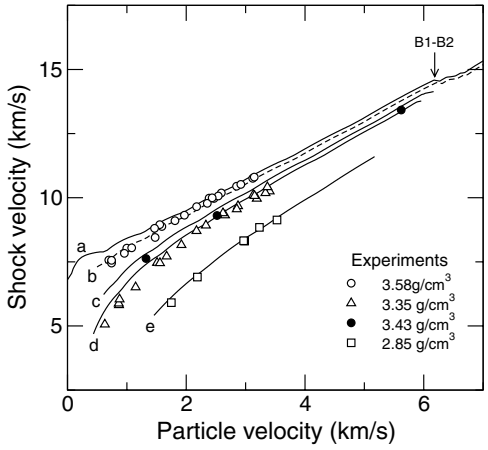

Figure 2. Comparison of the *ab fere initio* EOS with shock wave experiments in U_s–u_p space. Symbols represent experiments with various initial porosities [5–7]. Solid curves (a and c–e) denote simulations with initial porosities corresponding to experiments. Dashed curve b is a fictitious Hugoniot constructed with density 1% denser than the principal Hugoniot at the same shock pressure. The Hugoniot curves for porous material were truncated close to the lowest data point. At low pressures, the shock response of porous material is dominated by strength effects during compaction, and the snow-plough model adopted is no longer valid. Similarly, clean Hugoniot data are not obtained. Undulations evident in *a* at low velocities were caused by the use of bilinear interpolation in the EOS tables.

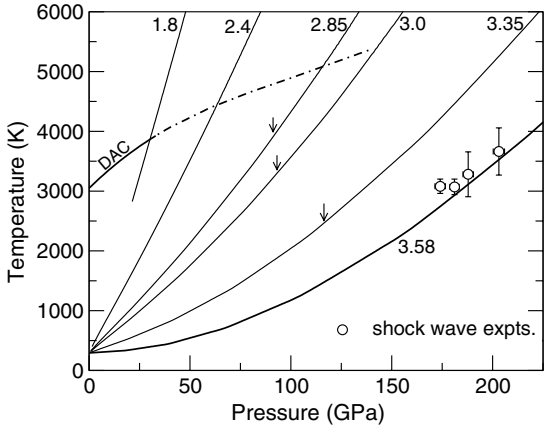

Figure 3. Predictions of the shock temperature on Hugoniots of different initial porosities (in P–T space) compared to measurements [8]. Numbers denote initial densities in g cm^{-3}. The DAC melting curve (solid) and its extrapolation (dot–dashed curve) follow [11]. Arrows indicate the (calculated) highest temperatures (pressures) achieved on the Hugoniots in experiments.

We also compared shock states for initially porous samples of periclase. For a given density in the shocked material, different shock temperatures (internal energies) can be achieved by varying the porosity of the starting material, thus probing thermodynamic space otherwise not readily accessible by shock experiments on full-density bulk material or by current DAC techniques. To predict the dynamic compression of porous periclase, we used a simplified form of a general model representing the strength of heterogeneous mixtures in continuum mechanics simulations [22, 23]. In the simplified model—which reduces to the 'snow-plough'

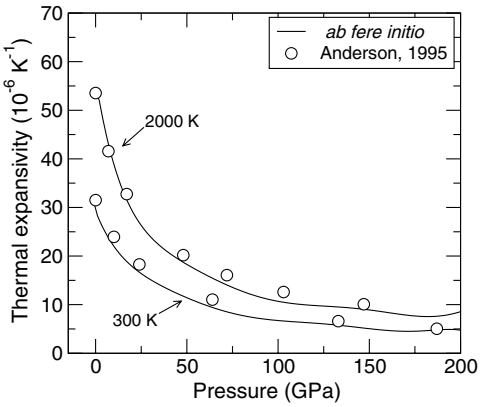

Figure 4. α versus P predicted from the *ab fere initio* EOS, compared to independent thermodynamic calculations based on measurements [25].

compaction model [24] for porous materials—the initial material was represented in the RH equations as a mixture of void and full-density solid at standard temperature and pressure. Shock states were calculated for compressions at least high enough to recompact fully—so the EOS of shocked material was void-free—and the material strength was ignored, which was a good approximation for pressures greater than 10 GPa or so. Shock wave experiments on MgO have been performed for starting materials with initial densities ranging from 2.85 to about 3.58 g cm^{-3} [5–8]. The predicted Hugoniots for porous periclase were in remarkable accord with experiments (figures 1, 2; only the Hugoniot with the highest porosity was shown in figure 1 for the sake of clarity), demonstrating again the accuracy of the *ab fere initio* EOS. Thus the EOS correctly predicted static and dynamic experimental results, and can be regarded as an accurate representation for the response of periclase. In the U_s–u_p plot (figure 2), the predictions deviate more from experiments at low pressures than high pressures, partly because of the limitations of the snow-plough model at low pressures where strength effects of the porous materials are dominant. The agreement is excellent at high pressures, with which we are more concerned. The shock temperatures on the porous Hugoniots were also computed from the *ab fere initio* EOS and the snow-plough model (figure 3).

Given the EOS, we calculated the volume thermal expansivity ($\alpha \equiv \partial \ln V/\partial T|_P$) as a function of pressure at various temperatures. The values of α predicted by our EOS were in excellent agreement with independent thermodynamic calculations [25] based on low pressure experimental data (figure 4) and previous *ab initio* calculations [12]. (As our EOS is in tabulated form, the calculated curve was less smooth than those calculated from analytic EOS [26].)

We also calculated the heat capacity at fixed volume ($C_V \equiv \partial E/\partial T\big|_V$) and at fixed pressure ($C_P \equiv \partial H/\partial T\big|_P$ where H is specific enthalpy) from the EOS (figure 5). C_P as a function of temperature at ambient pressure compares favourably to experiments [27], and is slightly higher than that in [12]. Also shown are two curves of $C_V(T)$ at $\rho = 3.56$ and 5.70 g cm^{-3} that approach to the Dulong–Petit value (49.86 J K^{-1} mol^{-1}) at high temperatures. Heat capacities represent the temperature gradients of energies. It would also be interesting to calculate the bulk sound speed at high pressures: $C_b \equiv \sqrt{(\partial P/\partial \rho)\big|_S}$ where S is specific entropy. As sound speed measurements are more tractable experimentally for shock waves than in DAC at megabar pressures, we calculated C_b on the principal Hugoniot (figure 5 inset). The calculated value at ambient pressure agrees with experiments [9].

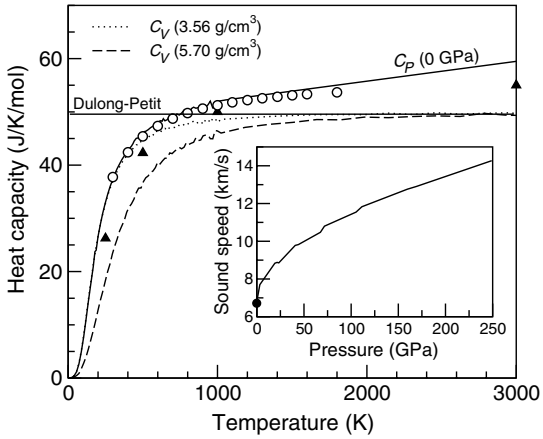

Figure 5. *Ab fere initio* EOS: heat capacity at fixed volume (C_V) and fixed pressure (C_P; 0 GPa) as a function of temperature. Circles are experimental values (C_P; 0 GPa) [27], and filled triangles values calculated by a different procedure [12]. Inset: bulk sound speed C_b on the principal Hugoniot. The filled circle denotes the experimental value [9].

A cold curve (e.g. EOS at electronic ground states and 300 K isotherm) or any reference state can be conveniently related to properties at different temperatures (energies and pressures) via the Grüneisen parameter:

$$\gamma(V, E) \equiv V \left.\frac{\partial P}{\partial E}\right|_V \approx V \left.\frac{P - P_0}{E - E_0}\right|_V \tag{1}$$

following a Mie–Grüneisen type equation of state. The Grüneisen parameter can also be defined in terms of thermal expansivity α or phonon frequency [25]. These definitions do not assume that γ is independent of temperature. The quasiharmonic assumption implies that γ for an individual phonon mode is independent of T. However, the population of vibrational modes with Bose–Einstein statistics is T-dependent, so the mean γ should be T-dependent in principle at least. Anharmonicity lends an additional temperature dependence to γ.

The finite difference approximation for γ given in equation (1) is accurate if the state concerned is close to the reference state, or if γ is independent of T and E. The latter was shown to hold for a variety of metals from shock wave experiments [20], though exceptions are not uncommon. For example, quantum mechanical calculations on bcc Ta [26] have shown strong T-dependence in γ. However, a popular empirical form is $\gamma = \gamma_0(V/V_0)^q$, where q is a dimensionless parameter [28]. This formulation is of great convenience for calculations related to the thermal contributions but are certainly not universal.

For MgO in the periclase structure, we calculated the Grüneisen parameter as a function of temperature, using the finite-difference approximation, as shown in figure 6. The Grüneisen parameter exhibited very weak temperature dependence. We found that $\gamma_0 \sim 1.45$ at ambient conditions, and that γ was not accurately represented by $\gamma = \gamma_0(V/V_0)^q$. This is similar to previous results [12] for EOS constructed by different techniques.

3. Phase transitions

The solid–liquid phase change above 50 GPa and the solid–solid (B1–B2) phase transition have not been documented experimentally for MgO, possibly because of technical limitations. The *ab fere initio* equation of state on the other hand indicates that such phase changes could

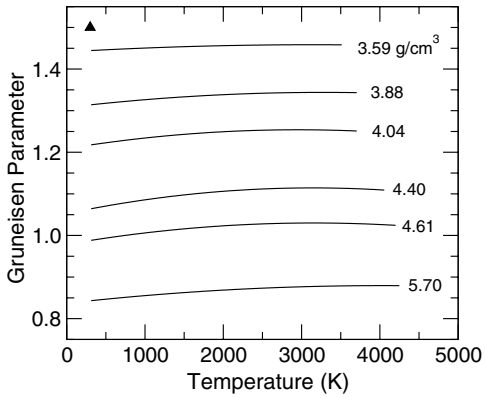

Figure 6. *Ab fere initio* EOS: γ versus T for various densities. The filled triangle is a separate calculation for ambient density [12].

be accessible by current experimental capabilities, by shock loading of periclase of different porosities to higher pressures and temperatures.

The melting of MgO is of extreme geophysical interest, and its melting point has been measured in DAC up to about 35 GPa [11], limited by heating difficulties from reaching higher melting temperatures at higher pressures. Melting curves from molecular dynamics simulations vary significantly, depending on the potential and technique adopted [2, 13]. Previous shock wave experiments on porous MgO explored temperatures significantly higher than the principal Hugoniot, but no indication of melting was observed in P–V and U_s–u_p space. This observation is consistent with the extrapolated melting curve from DAC experiments [11], as the highest-temperature states (indicated by arrows in figure 2) achieved on these experimental Hugoniots lie below the predicted equilibrium melting curve. If the extrapolated DAC melting curve [11] is valid, melting is expected to occur at about 63 and 114 GPa on the porous Hugoniots with initial densities of 2.4 and 2.85 g cm^{-3}, respectively, assuming equilibrium melting. If superheating exists [29, 30], the temperature at the transition should be regarded as the upper bound of the melting point at the corresponding pressure. Besides shock wave experiments, a more realistic interatomic potential may be developed based on our EOS, and the melting curve may be simulated more accurately with molecular dynamics.

Similar techniques can, in principle, be applied to investigate the B1–B2 phase boundary. Current EOS predict that the B1–B2 transition occurs at about 270 and 324 GPa on Hugoniots with initial densities of 3.35 and 3.58 g cm^{-3}, respectively, assuming equilibrium behaviour. Although it is possible that this phase change is not accessible for conventional shock wave loading, and melting may occur before the B1–B2 transition, experiments on porous periclase may determine pressure and temperature bounds for the phase boundary.

4. Conclusion

A thermodynamically complete *ab initio* equation of state of MgO was obtained using density functional theory and the quasiharmonic phonon approximation, and adjusted to match the observed ambient density. This equation of state is in remarkable agreement with static and shock wave experiments including shock temperatures. The Grüneisen parameter of periclase was shown to be weakly dependent on temperature. Using this EOS, we predict that the

melting curve of MgO at the Earth's lower mantle pressures should be accessible by shock wave loading of porous periclase, which could also put pressure and temperature bounds on the B1–B2 transition.

Acknowledgments

SNL is sponsored by a Director's Postdoctoral Fellowship at LANL (groups P-24 and EES-11). This work was performed in part under the auspices of US Department of Energy under contract No W-7405-ENG-36.

References

[1] Karki B B, Stixrude L and Wintzcovich R M 1997 *J. Phys.: Condens. Matter* **9** 8579
[2] Strachan A, Çağin T and Goddard W A III 1999 *Phys. Rev.* B **60** 15084
[3] Karki B B, Stixrude L and Wintzcovich R M 2001 *Rev. Geophys.* **39** 507
[4] Drummond N D and Ackland G J 2002 *Phys. Rev.* B **65** 184104
[5] Al'tshuler L V, Trunin R F and Simokov G V 1965 *Izv. Akad. Nauk SSSR Fiz. Zemli* **10** 1
[6] van Thiel M 1977 *Compendium of Shock Wave Data (UCRL-50108)* vol 2(A2) (Livermore: Lawrence Livermore Laboratory) p 405
[7] Marsh S P 1981 *LASL Shock Hugoniot Data* (Berkeley, CA: University of California Press)
[8] Svendsen B and Ahrens T J 1987 *Geophys. J. R. Astron. Soc.* **91** 667
[9] Jackson I and Niesler H 1982 *High Pressure Research in Geophysics* (Tokyo: Center for Academic Publishing) p 93
[10] Duffy T S, Hemley R J and Mao H K 1995 *Phys. Rev. Lett.* **74** 1371
[11] Zerr A and Boehler R 1994 *Nature* **371** 506
[12] Oganov A R and Dorogokupets P I 2003 *Phys. Rev.* B **67** 224110
[13] Belonoshko A B and Dubrovinsky L S 1996 *Geochim. Cosmochim. Acta* **60** 1645
[14] Swift D C, Ackland G J, Hauer A and Kyrala G A 2001 *Phys. Rev.* B **64** 214107
[15] Payne M C, Teter M P, Allan D C, Arias T A and Joannopoulos J D 1992 *Rev. Mod. Phys.* **64** 1045
[16] Vanderbilt D 1990 *Phys. Rev.* B **41** 7892
[17] Monkhorst H J and Pack J D 1977 *Phys. Rev.* B **16** 2981
[18] Akbarzadeh H, Clark S J and Ackland G J 1993 *J. Phys.: Condens. Matter* **5** 8065
[19] Poirier J-P 1991 *Introduction to the Physics of the Earth's Interior* (Cambridge: Cambridge University Press) p 58
[20] McQueen R G, Marsh S P, Taylor J W, Fritz J N and Carter W J 1970 *High Velocity Impact Phenomena* (New York: Academic) p 294
[21] Luo S-N, Akins J A, Ahrens T J and Asimow P D 2004 *J. Geophys. Res.* **109** B05205
[22] Swift D C and Mulford R N 2004 personal communication
[23] Wang Y, Ahuja R and Johansson B 2002 *Shock Compression of Condensed Matter-2001* (*AIP Conf. Proc.* vol 620) (Melville, NY: American Institute of Physics) p 67
[24] Herrmann W 1969 *J. Appl. Phys.* **40** 2490
[25] Anderson O L 1995 *Equations of State of Solids for Geophysics and Ceramic Science* (New York: Oxford University Press)
[26] Cohen R E and Gülseren O 2001 *Phys. Rev.* B **63** 224101
[27] Robie R A, Hemingway B S and Fisher J S 1979 *Thermodynamic Properties of Minerals and Related Substances at 298.15 K and 1 Bar (*10^5 *Pascals) Pressure and at High Temperatures* (Washington, DC: US Government Printing Office) p 184
[28] Anderson O L 1979 *J. Geophys. Res.* **84** 3537
[29] Luo S-N and Ahrens T J 2003 *Appl. Phys. Lett.* **82** 1836
[30] Luo S-N, Ahrens T J, Çağin T, Strachan A, Goddard W A III and Swift D C 2003 *Phys. Rev.* B **68** 134206